MESOSCALE MODELING OF FRAGMENTATION OF CERAMICS UNDER DYNAMIC COMPRESSIVE LOADING

P. H. Geubelle, S. Maiti and K. Rangaswamy
Department of Aerospace Engineering, University of Illinois, Urbana, IL 61801 USA

ABSTRACT

We present the results of a numerical analysis of ceramics under dynamic compressive loading conditions. The analysis is performed at the mesoscale level using a grain-based finite element scheme that accounts for the granular microstructure of the material. An explicit cohesive/volumetric finite element scheme is used to simulate the constitutive and failure response of the ceramic specimen subjected to uniform or impact-induced compressive loading. In this analysis, failure is assumed to be of intergranular nature, i.e., the cohesive elements are placed along the grain boundaries. A rate-independent, damage-dependent cohesive failure model is used to characterize the progressive failure of the cohesive surfaces. Coupling between normal and shear failure is achieved by expressing the normal and tangential components of the cohesive traction vector in terms of the L_2 norm of the non-dimensionalized displacement jump vector. Contact between the fracture surfaces and between the fragments is captured through a combination of a cohesive-based and minimization-based contact enforcement schemes. The damage evolution during the fragmentation process is characterized in terms of two different and complementary damage parameters: the first one denotes the appearance and propagation of the distributed damage (or micro-cracks) as cohesive surfaces progressively fail under the effect of the dynamic loading conditions; the second one characterizes the coalescence of the micro-cracks and the creation of fragments. Special emphasis is placed in this paper on the analysis of the frictional contact effect on the initiation, propagation and final extent of the fragmentation process. A detailed parametric analysis is performed to study how the value of the friction coefficient affects the energy absorption process associated with the fragmentation event under various strain rate levels and for different grain sizes.

1 INTRODUCTION

Most of the existing theoretical and numerical analyses of fragmentation of ceramic materials rely on continuum homogenized properties and focus on the tensile loading case (Grady [1], Drugan [2] and Miller *et al.* [3]). The objective of the present study is to investigate numerically the evolution of damage in a ceramic specimen subjected to a uniform initial state of high strain rate compressive loading, and to perform this analysis at the mesoscale level, i.e., by taking into account the granular microstructure of the material. Related studies on the topic can be found in the finite element investigations conducted by Espinosa *et al.* [4] and by Zavattieri and Espinosa [5]. This paper constitutes an extension to the compressive regime of a recent study performed by the authors on the mesoscale simulations of ceramics subjected to dynamic tensile conditions (Maiti *et al.* [6]). Although it relies on similar numerical tools and assumptions, the analysis summarized hereafter presents a major difference with the tensile case: under compressive loads, the failure process is quite different and involves a mode change to a shear-dominated failure. Therefore, the frictional contact taking place, first, between the surfaces of the micro-cracks and, then, between the fragments is expected to play an important role in the evolution and final extent of damage. The frictional effect on the fragmentation process constitutes the main topic of this paper, which starts with a summary of the numerical scheme and a description of the problem

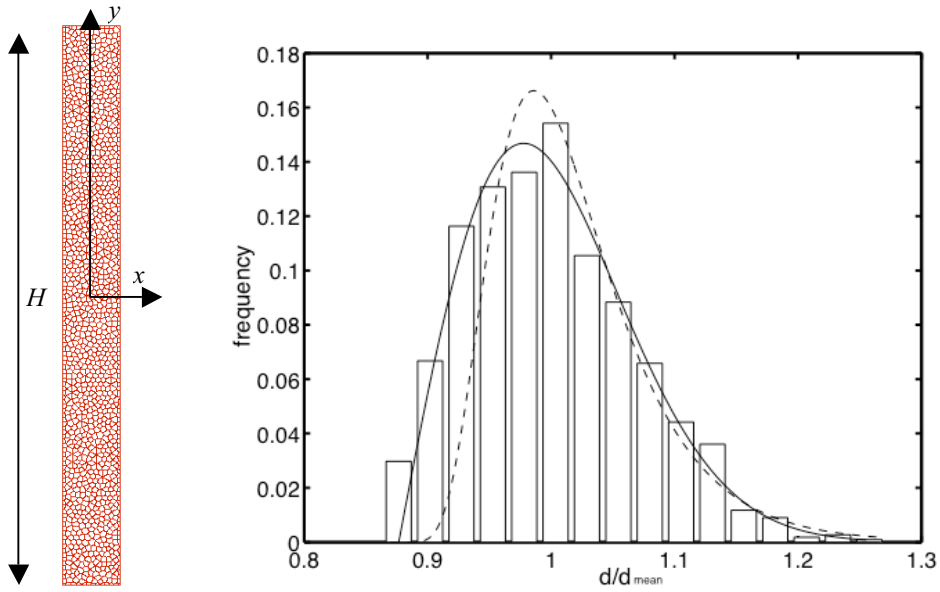

Figure 1 Problem geometry (left) and typical grain size distribution (right), compared with the log-normal (dashed) and generalized Louat (solid curve) distributions. *d* denotes the grain size.

solved (Section 2), then presents the key features of the fragmentation process and the results of a parametric study of the effects of the friction coefficient on the damage evolution (Section 3).

2 PROBLEM DESCRIPTION AND NUMERICAL SCHEME

The problem to be investigated hereafter is presented in Figure 1. It consists of a thin ceramic specimen of length H and width $W=H/10$ composed of a large number of grains and subjected to an uniform state of uniaxial compression applied through the following initial velocity field:

$$v_x(x,y,0)=0, \quad v_y(x,y,0)=-\dot{\varepsilon}_o y, \quad -\frac{W}{2}\le x\le\frac{W}{2} \text{ and } -\frac{H}{2}\le y\le\frac{H}{2}, \tag{1}$$

where $\dot{\varepsilon}_o$ denotes the initial strain rate, and the following velocity boundary conditions along the top and bottom edges of the domain:

$$v_x\left(x,\frac{\pm H}{2},t\right)=0, \quad v_y\left(x,\frac{\pm H}{2},t\right)=\mp\dot{\varepsilon}_o\frac{H}{2}, \quad -\frac{W}{2}\le x\le\frac{W}{2} \text{ and } t>0. \tag{2}$$

The left and right edges are traction free. As illustrated below, the presence of traction-free conditions along the sides of the specimen play an important role in the evolution and final extent of damage. Future studies will focus on the effect of lateral confinement. Various grain sizes are considered, with an average grain size d_{mean} ranging from 1 to 100 μm.

The three key assumptions behind the analysis presented hereafter are 1) the analysis is performed in 2-D under plane strain conditions; 2) the failure takes place in an intergranular fashion, i.e., we assume that the grain boundaries are much weaker than the individual grains; and 3) the constitutive response of the grains is assumed to be linearly elastic and isotropic. The domain is discretized with a combination of volumetric and cohesive elements (Maiti and Geubelle, [7]). 3-noded constant strain triangular volumetric elements are used to capture the bulk constitutive response of individual grains, while 4-noded interfacial (cohesive) elements are placed along the grain boundaries. The response of the cohesive elements is described by a mixed-mode, rate-independent, damage-dependent bilinear cohesive failure law between the normal and

tangential components of the cohesive traction vector $\mathbf{T} = (T_n, T_t)$ and the corresponding displacement jump vector $\boldsymbol{\Delta} = (\Delta_n, \Delta_t)$:

$$T_n = \frac{S}{1-S}\frac{\sigma_{\max}}{S_{init}}\frac{\Delta_n}{\Delta_{nc}}, \quad T_t = \frac{S}{1-S}\frac{\tau_{\max}}{S_{init}}\frac{\Delta_t}{\Delta_{tc}}, \tag{3}$$

where $\sigma_{\max}$ and $\tau_{\max}$ respectively denote the tensile and shear strength of the grain boundaries, Δ_{nc} and Δ_{tc} are the critical values of the normal and tangential displacement jumps across the cohesive surfaces, and S is the monotonically decreasing damage parameter related to the L_2 norm of the normalized displacement jump vector $\tilde{\boldsymbol{\Delta}} = (\Delta_n / \Delta_{nc}, \Delta_t / \Delta_{tc})$:

$$S = \left\langle 1 - \left\| \tilde{\boldsymbol{\Delta}} \right\| \right\rangle, \tag{4}$$

with $\langle a \rangle = a$ if $a \geq 0$ and $= 0$ otherwise. In eqn (3), S_{init} denotes the initial value of S chosen close to unity (typically 0.98).

Details on the numerical scheme can be found in (Maiti *et al.* [6]). For completeness, let us indicate here that it involves a nonlinear kinematics description of the motion to account for the possible large rotations of fragments during the fragmentation process. A frictional cohesive contact algorithm incorporated in the cohesive failure law (3) is used to capture the contact between the surfaces of the micro-cracks detection during the initial phase of the failure process. It is followed by a more general two-step non-smooth contact scheme to model the inter-fragment contact, once large relative motion between initially adjacent grains has taken place. Finally, the numerical scheme relies on an explicit time stepping scheme to capture the complex dynamic fracture process in the specimen.

To quantify the evolution of the damage process throughout the fragmentation event, we use two complementary damage parameters. The first one, referred to as the *damage index* (DI), is defined as the relative proportion of cohesive elements that have failed and is a measure of the distributed damage in the specimen. The second one, referred to as λ, corresponds to the total number of fragments divided by the total area of the specimen, i.e., is the number of fragment per unit area (in mm^{-2}). This second parameter denotes the creation of individual fragments associated with the coalescence of the distributed microcracks.

3 DAMAGE EVOLUTION

In all the simulations presented hereafter, the normal and shear failure strength values are $\sigma_{\max} = \tau_{\max} = 1\ GPa$, the mode I and mode II fracture toughnesses are also assumed to be equal

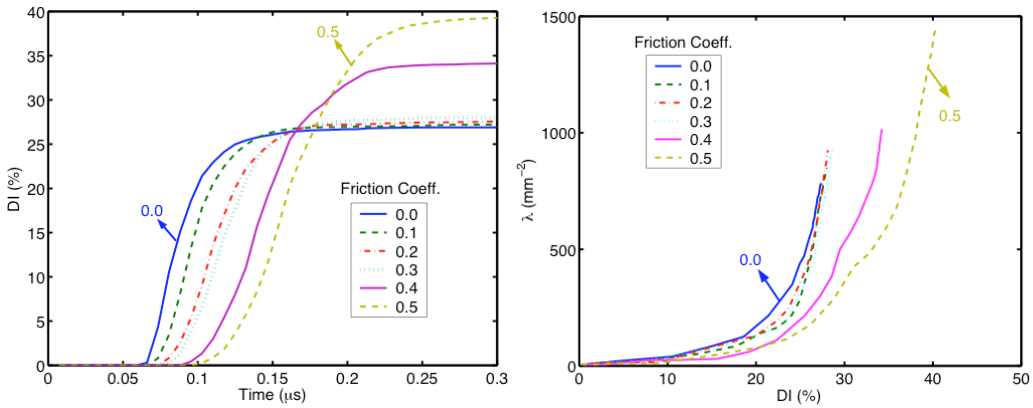

Figure 2 : Effect of the friction coefficient on the evolution of the damage parameter *DI* (left) and on the λ vs. *DI* curves (right) for a specimen with a 10 μm average grain size.

$G_c = \sigma_{\max}\Delta_{nc}/2 = \tau_{\max}\Delta_{tc}/2 = 69.5\ J/m^2$, and the average grain size is $10\ \mu m$. The ceramic specimen is made of alumina, with a Young's modulus $E = 400\ GPa$, a Poisson's ratio $\nu = 0.27$ and a density $\rho = 3800\ kg/m^3$. Figure 2 presents the effect of the friction coefficient μ on the evolution of damage index *DI*. While all curves present a similar trend, some notable differences are observed. Firstly, the friction coefficient affects the failure initiation time, and therefore the amount of energy stored in the grains and available for fragmentation. The final damage (i.e., the final value of *DI*) is therefore more important for high values of μ, but this dependence on the friction coefficient is clearly nonlinear: while no noticeable changes are observed for $0 \le \mu \le 0.3$, substantial changes are observed for the two largest values of μ ($\mu = 0.4$ and 0.5). There appears to be also a change in the rising part of the *DI vs*. time curves for these two higher values of μ, with a more progressive increase that that observed for the lower values of μ. This transition is also apparent in the *DI* vs. λ curves, which relate distributed micro-cracking to the formation of discrete fragments. In all cases, substantial micro-cracking must take place before the formation of fragments. However, for low values of the friction coefficient, all curves seem to overlap indicating a similar fragmentation pattern. For $\mu = 0.4$ and 0.5, fragmentation appears to take place for higher values of *DI*, and the final number of fragments is much higher.

To understand this transition process, we present in Figure 3 three snapshots of the damage process in the specimen obtained for $\mu = 0$ (Fig. 3a-c) and $\mu = 0.5$ (Fig. 3d-f). Inn each case, the first two figures present the damage distribution plotted on the undeformed configuration for similar values of *DI*, while the third one shows the final deformed shape of the specimen. In both

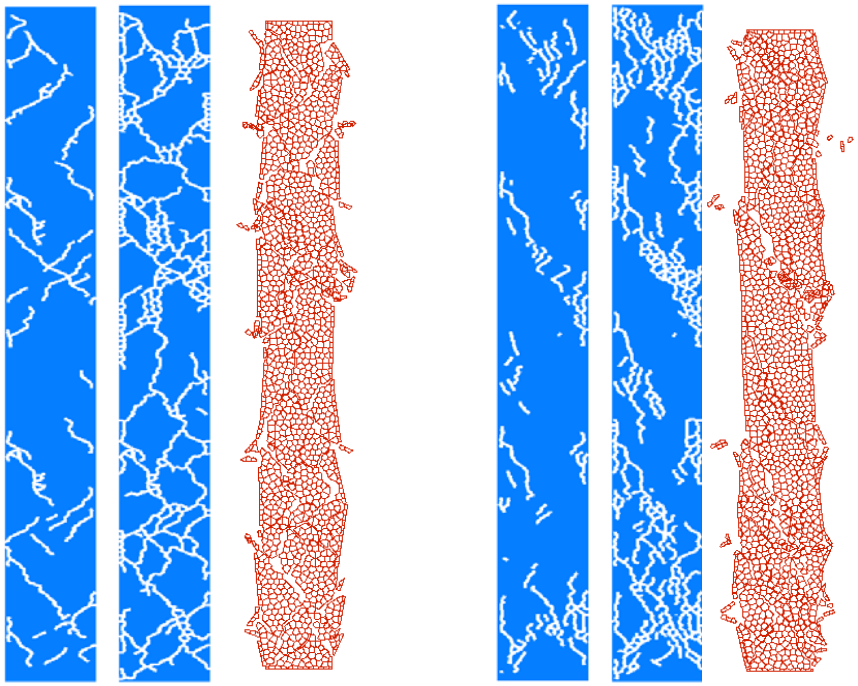

Figure 3. Effect of the friction coefficient μ on the evolution of the damage process. (a-c) : $\mu = 0$, (d-f) : $\mu = 0.5$. Fig. (a) and (d) : $DI = 0.10$. Fig. (b) and (e) : $DI = 0.27$. Fig. (c) and (d) show the dinal damage on the deformed specimen configuration.

cases, the failure mode conversion to shear-dominated failure along inclined cohesive surfaces is clearly apparent. However, while the damage seems to be more distributed for the case $\mu = 0$, it tends to be more localized in bands in the case $\mu = 0.5$. The fragment size is also observed to be much smaller for the higher value of the friction coefficient, although some very large fragments are present due to the presence of localized failure bands.

The difference between the two failure modes is also visible in the resulting average stress-strain curves (Figure 4). The average stress is computed by monitoring the vertical reaction along the top and bottom edges of the domain and diving these by the domain width W. Due to inertial effects, the stress values extracted from the top and bottom vertical reactions are slightly different, although the general shape of the stress-strain curves is very similar. In all cases, the curve is initially linear, reaches a maximum, and then follows a progressive downward trend associated with compressive resistance of the sliding fragments. The additional strength due to frictional contact between the fracture surfaces is clearly visible, with an increase in strength exceeding 80% between $\mu = 0$ and $\mu = 0.5$. This effect is expected to be reinforced in the presence of lateral confinement, which constitutes the main topic of the current phase of this research project.

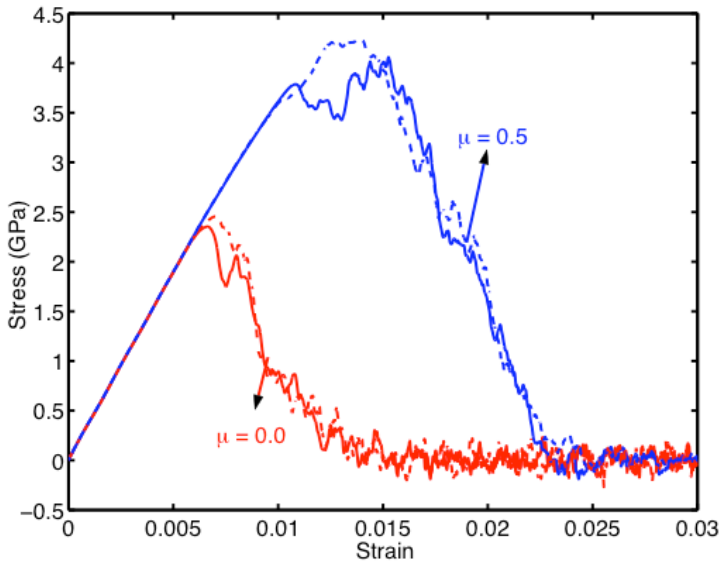

Figure 4 : Effect of the friction coefficient μ on the computed stress-strain relation. The solid and dashed curves respectively correspond to the values obtained from vertical reactions along the top and bottom edges.

ACKNOWLEDGEMENT

This research project was partially funded by NSF through the Career Award CMS-9734473.

REFERENCES

[1] D. E. Grady. Local inertial effects in dynamic fragmentation. *J. Appl. Phys.*, 53(1):322-325, 1982.

[2] W. J. Drugan. Dynamic fragmentation of brittle materials: analytical mechanics-based models. *J. Mech. Phys. Solids*, 49:1181-1208, 2001.

[3] O. Miller, L. B. Freund, and A. Needleman. Modeling and simulation of dynamic fragmentation in brittle materials. *Int. J. Fract*., 96:101-125, 1999.

[4] H. D. Espinosa, P. D. Zavattieri, and S. K. Dwivedi. A Finite deformation continuum/discrete model for the description of fragmentation and damage in brittle materials. *J. Mech. Phys. Solids*, 46(10):1909-1942, 1998.

[5] P. D. Zavattieri and H. D. Espinosa. Grain level analysis of crack initiation and propagation in brittle materials. *Acta Mater*., 49(20):4291-4311, 2001.

[6] S. Maiti, K. Rangaswamy, and P. H. Geubelle. Mesoscale analysis of dynamic fragmentation of ceramics under tension. Submitted to *Acta. Mater.*, 2004.

[7] S. Maiti and P. H. Geubelle. Mesoscale modelling of dynamic fracture of ceramic materials. *Comp. Meth. Engr. Sci*., 5(2):91-102, 2004.